Crystallographic tilt in Lateral Overgrowth of GaN epitaxial layers
--- mask material dependence ---

S. Tomiya [a)*], T. Hino[b)], S. Kijima [b)], T. Asano [b)], H. Nakajima [c)], K. Funato [c)], T. Asatsuma [c)], T. Miyajima [c)], K. Kobayashi [c)] and M. Ikeda [b)]

a) Environment and Analysis Technology Department, Technical Support Center, Sony Corporation, 2-1-1, Shin-Sakuragaoka, Hodogaya, Yokohama 240-0036, Japan

b) Development Center, Sony Shiroishi Semiconductor Inc., 3-53-2 Shiratori, Shiroishi-shi, Miyagi-ken 989-0734, Japan

c) Semiconductor Laser Division, Semiconductor Company, Core Technology and Network Company, Sony Corporation, 2-1-1, Shin-Sakuragaoka, Hodogaya, Yokohama 240-0036, Japan

* E-mail Address: Shigetaka.Tomiya@jp.sony.com

For epitaxial growth of GaN and other III-V nitrides, sapphire and silicon carbide substrates have been mainly used, since there is presently no suitable alternative. However, due to the large lattice mismatch and difference between the thermal-expansion coefficients of GaN and these substrate materials, a high density of dislocations (typically 10^8 – 10^{10} cm^{-2}) is inevitable. Lateral growth technique has been applied to the epitaxial growth of GaN to minimize dislocation density [1-8]. However, crystallographic tilt in lateral growth regions (wing regions) occurred and this may affect the optical properties of the GaN layer and are detrimental to the fabrication of high performance and high reliability optical devices.

We have investigated the dependence of crystallographic tilt and defect distribution on mask material in lateral overgrowth of GaN epitaxial layers using x-ray diffraction and transmission electron microscopy (TEM).

Epitaxial lateral overgrown (ELO) GaN layers were grown by atomspheric pressure metalorganic chemical vapor deposition (MOCVD). We prepared five different masks: an electron beam (EB)-evaporated silicon dioxide (SiO_2) mask, a plasma enhanced chemical vapor deposition (PECVD)-grown SiO_2 mask, a PECVD-grown silicon nitride (SiN_x) mask and a layered PECVD SiN_x /PECVD SiO_2. The thickness of the mask was about 200nm. Layered masks consist of 10nm-thick SiN_x on 200nm-thick SiO_2. Stripes in ELO GaN layers were aligned in the $<1\bar{1}00>$ direction.

Figure 1 shows X-ray rocking curves (XRCs) of the (0004) ω-scan for ϕ=0º and ϕ=90º, where the azimuth ϕ is the angle between the stripe direction and the rotation axis of ω scan. Three diffraction peaks are observed for ϕ=0º when the mask material is EB SiO_2 (Fig.1(a)), while splitting of the diffraction peak is not observed for ϕ=0º in case of other mask materials. The results indicate that crystallographic tilt in an ELO GaN layer was suppressed by changing the mask material from EB-SiO_2 to PECVD-SiO_2 and PECVD SiN_x. In the case of the PECVD SiO_2, the full width at half-maximum (FWHM) of the main peak for ϕ=0º also became narrower than when the EB SiO_2 mask is used. The ratio of the FWHM for ϕ=0º to that of for ϕ=90º is almost unity and are smallest when the PECVD SiN_x, and PECVD SiN_x/PECVD SiO_2.

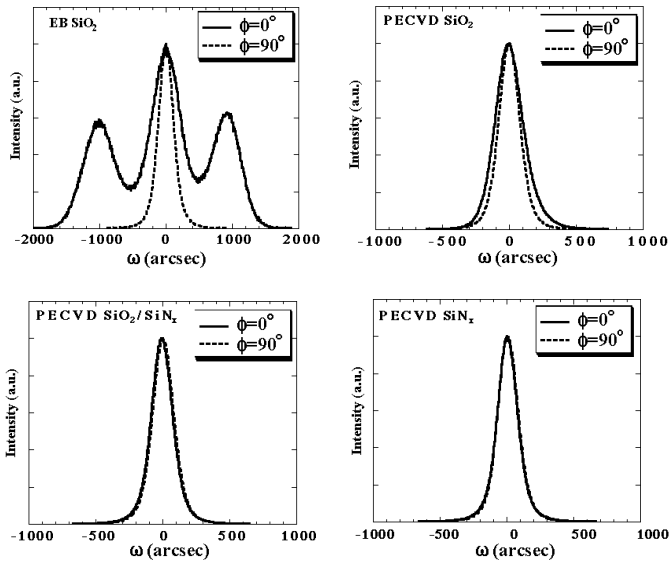

FIG. 1 X-ray rocking curves of the GaN (0004) peak for ELO GaN with (a) EB SiO_2 mask, (b) PECVD SiO_2 mask, (c) PECVD SiN_x mask, and (d) PECVD SiN_x/PECVD

Figure 2 shows cross sectional TEM images of a coalescence site in the wing region of ELO GaN layer with EB SiO_2 mask taken

with different reflection vectors **g**. Two different types of dislocations are observed in the images. Many small dislocation fragments were piled up along the c-axis in Fig. 2(b), while dislocations originating from the coalescence site on the mask propagated along the c-axis in Fig. 2(b). The former type and latter type of dislocations are referred here to as type I dislocations and type II dislocations, respectively. Based on the contrast-invisibility criterion, i.e., $\mathbf{g}\cdot\mathbf{b}=0$, the type I dislocations have Burgers vector $\mathbf{b}=1/3\langle 11\bar{2}0\rangle$ and the type II dislocations have Burgers vector $\mathbf{b}=\langle 0001\rangle$. The type II dislocations in Fig. 2 (b) are pure screw dislocations. Some type II dislocations have Burgers vector $\mathbf{b}=1/3\langle 11\bar{2}3\rangle$ and thus are mixed dislocations. An important feature of the type II dislocations is that their Burgers vectors have a c-plane component.

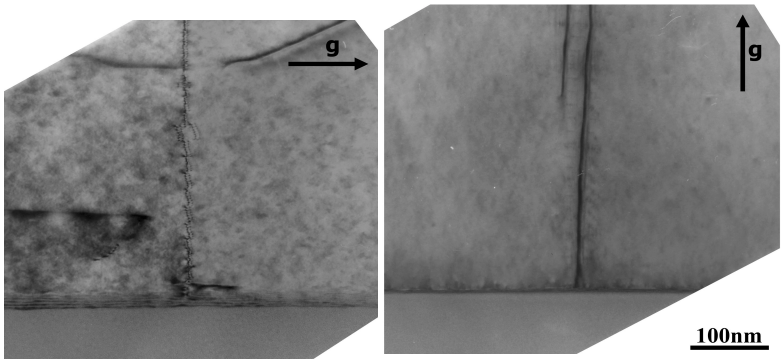

FIG.2 Close-up cross sectional TEM images of a coalescence site of ELO GaN layer with EB SiO_2, viewed with (a) $\mathbf{g}=11\bar{2}0$ and (b) $\mathbf{g}=0002$.

The piling up of dislocations (type I dislocations) along the c-axis is also observed above the edges of mask in the case of EB SiO_2 mask. The type I dislocations were not observed in ELO GaN layers with other mask materials. Thus, appearance of the type I dislocations is correlated to c-axis tilt in the wing region of ELO GaN layers. Type II dislocations are also observed at the coalescence sites of the ELO GaN layers with PECVD SiO_2 mask. On the other hand, no or few type II dislocations were observed at the coalescence site of the ELO GaN layers with the PECVD SiN_x mask and the PECVD SiN_x/PECVD SiO_2. The FWHM of the (000*l*) ω-scan XRC peak is broadened by pure screw and/or mixed threading dislocations content in the GaN film on saphire [9]. Thus, the appearance of the type II dislocations is correlated with the broadening of the (0004) XRC peaks, as seen in Fig.1.

As we described here, crystallographic tilt and defect distribution in ELO GaN layers changes in accordance with mask materials. It is important to note that by depositing a thin PECVD SiN_x layer on the PECVD SiO_2, the crystalline quality of the ELO GaN layers changes from that used with the SiO_2 mask to that used with SiN_x mask. These results suggest that the interface between the ELO GaN layer and the mask has a significant effect on crystallographic tilt and defect distribution. We will present effects on growth conditions and will also present crystallographic tilt and defect distribution of GaN layers by Pendeo epitaxy technique [10], which is recently used with our laser structure [11], by comparing with crystalline quality of ELO GaN layers. We finally discuss the mechanism of crystallographic tilt in the lateral overgrowth of GaN.

References

[1] T. S. Zheleva, O.H. Nam, M.D. Bremser and R F. Davis, Appl. Phys. Lett., **71**, 2472, (1997)
[2] O. H. Nam, M. D. Bremser, T. S. Zheleva, and R. F. Davis, Appl. Phys. Lett., **71**, 2638 (1997)
[3] Y. Kato, S. Kitamura, K. Hiramatsu and N. Sawaki, J. Crystal. Growth, **144**, 133 (1994)
[4] S. Kitamura, K. Hiramatsu and N. Sawaki, Jpn. J. Appl. Phys., **34**, L1184 (1995)
[5] A. Usui, H. Sunagawa, A. Sakai, and A. Yamaguchi, Jpn. J. Appl. Phys., **36**, L899 (1997)
[6] A. Sakai, H. Sunakawa and A. Usui, Appl. Phys. Lett., **71**, 2259 (1997)
[7] H. Marchand, X. H. Wu, J. P. Ibbetson, P. T. Fini, P. Kozodoy, S. Keller, J. S. Speck, S. P. DenBaars, and U. K. Mishra, Appl. Phys. Lett., **73**, 747 (1998)
[8] A. Sakai, H. Sunakawa and A. Usui, Appl. Phys. Lett., **73**, 481 (1998)
[9] B. Heying, X. H. Wu, S. Keller, Y. Ki, D. Kapolnek, B.P. Keller, S. P. DenBaars, and J. S. Speck, Appl. Phys. Lett., **68**, 643 (1996).
[10] O.H.Nam, M.D.Bremser, T.Zheleva, and R.F.Davis, Appl. Phys. Lett., **71**, 2638 (1997)
[11] S. Uchida, S. Kijima, T. Tojyo, S.Ansai, M.Takeya, T.Hino, K.Shibuya, S.Ikeda, T.Asano, K.Yanashima, S.Hashimoto, T.Asatsuma, M.Ozawa, T.Kobayashi, Y.Yabuki, T. Aoki and M.Ikeda, SPIE, San Jose (1999)